Detection Efficiency of Plastic Scintillator for Neutron Energies 4 to 76 Mev*

CLYDE E. WIEGAND, TOM ELIOFF, WILLIAM B. JOHNSON, LEONARD B. AUERBACH, JOSEPH LACH, AND THOMAS YPSILANTIS
Lawrence Radiation Laboratory, University of California, Berkeley, California

(Received February 5, 1962)

The neutron detection efficiency of plastic scintillator counters 15 cm thick has been determined for neutron energies from 4 to 76 Mev. Neutrons in this energy range were obtained by scattering a 205-Mev neutron beam from a hydrogen target. A proton-range telescope selected the forward-scattered protons from the n-p reaction, thus monitoring the flux of monoenergetic neutrons scattered in a prescribed direction. Near 10 Mev the efficiency is 30%, and it slowly decreases to 20% at 76 Mev.

I. INTRODUCTION

THE design of many types of neutron detectors[1] depends upon such factors as the neutron energy of interest, the detection efficiency, and the speed of response. Many types of organic and inorganic scintillators can be found for various neutron counting applications.[2,3] However, for neutron energies greater than about 1 Mev, the scintillation counter offers a relatively simple, efficient, and fast detector. One of the principal problems existing in the use of such a counter for the detection of proton recoils is the determination of its detection efficiency.

The efficiency of plastic scintillators for counting neutrons has been studied by many workers for neutron energies below 14 Mev and for scintillator thicknesses of the order of 5 cm.[4–7] Here we report on the efficiency of plastic scintillator blocks 15 cm thick, used for counting neutrons in the energy range of 4 to 76 Mev. The plastic scintillator is $\approx 97\%$ polystyrene, $\approx 3\%$ terphenyl, and 0.03% tetraphenyl butadiene. This composition has about equal numbers of hydrogen and carbon atoms.

This efficiency measurement was necessary for our study of the reaction $\pi^{\mp}+p \rightarrow \pi^{+}+\pi^{\mp}+n$. The apparatus used to observe this process consisted of a spherical array of 84 scintillation counters covering π steradians at a 5-ft radius. The plastic scintillator for each of these counters was 15 cm thick, and varied in the other dimensions from 20 by 10 cm to 20 by 80 cm. Since time-of-flight was used to distinguish the neutron from the pions in the above process, it was necessary to determine the time distribution of phototube pulses from neutrons of a given energy as well as to determine their detection efficiency.

Below 10 Mev and for plastic scintillators up to 5 cm thick, calculated neutron efficiencies are in agreement with those experimentally determined.[4,5,7] One can obtain fair agreement by considering only single n-p collisions while ignoring the carbon content of the scintillator. However, at energies greater than 10 Mev the neutron interactions with carbon become important.

Our method of measuring the neutron efficiency utilized the neutron beam from the Lawrence Radiation Laboratory 184-in. cyclotron. The neutrons impinged on a hydrogen target. A proton-range telescope selected the forward-scattered protons from the n-p reaction, thus monitoring the number of monoenergetic neutrons scattered in a given direction.

II. EXPERIMENTAL ARRANGEMENT

The experimental setup outside of the cyclotron shielding is shown in Fig. 1. Neutrons were stripped from 450-Mev deuterons incident on a copper target within the cyclotron. At a distance of 30 ft from the cyclotron, the neutrons passed through a steel collimator $1\frac{1}{2}$ in. high by $1\frac{1}{4}$ in. wide by 5 ft long. The liquid-hydrogen target was positioned beyond the collimator. A sweeping magnet was stationed between the collimator and the hydrogen target to remove charged particles from the beam.

The position and size of the neutron beam were checked by placing a hydrogenous material immediately in front of an x-ray film at the hydrogen-target position. The film verified that the neutron-beam position and size were determined by the position and dimensions of the collimator.

Liquid hydrogen was contained in a 4-in.-diam Mylar container with 0.007-in. walls. The outer vacuum jacket of the target was an aluminum sphere of $\frac{1}{8}$-in. thickness except for the entrance and exit windows which were also 0.007-in. Mylar. The whole target apparatus was mounted on rails so that the target could be temporarily moved aside. A transit could then be placed at the position normally occupied by the target in order to accurately determine the scattering angle of the proton (θ_p) and of the neutron (θ_n).

The proton-range telescope was formed by the scintillation counters S_1, S_2, S_3, and S_4, together with the copper absorbers A_1 and A_2. The S_2 counter was geometrically de-

* Work done under the auspices of the U. S. Atomic Energy Commission.

[1] B. Rossi and H. Staub, *Ionization Chambers and Counters* (McGraw-Hill Book Company, Inc., New York, 1949), pp. 135–185.
[2] J. B. Birks, *Scintillation Counters* (Pergamon Press, New York, 1960), p. 111.
[3] W. D. Allen, *Neutron Detection* (Philosophical Library, Inc., New York, 1960), p. 72.
[4] H. Grassler and K. Tesch, Nuclear Instr. & Methods **10**, 353 (1961).
[5] J. Hardy, Rev. Sci. Instr. **29**, 705 (1958).
[6] L. Cranberg and J. Levin, Phys. Rev. **103**, 343 (1956).
[7] R. Batchelor, W. B. Gilboy, J. B. Parker, and J. H.Towle, Nuclear Instr. & Methods **13**, 70 (1961).

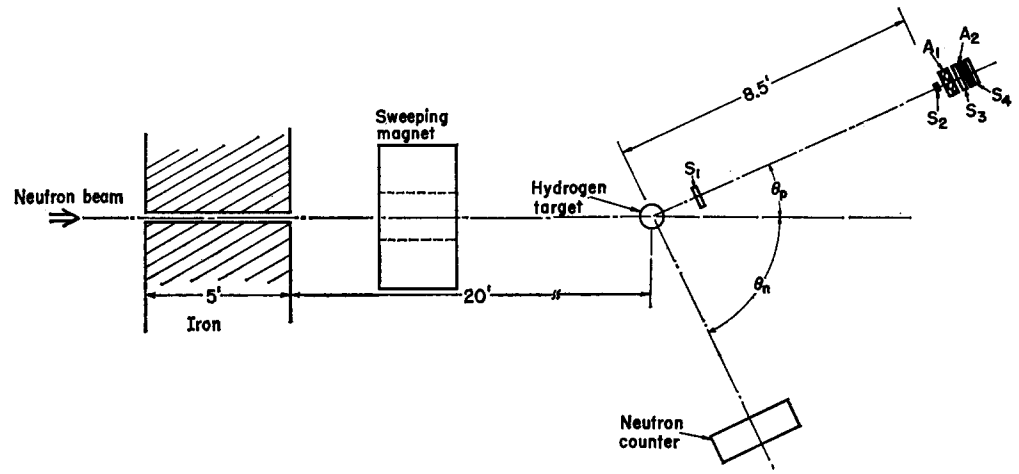

FIG. 1. Schematic diagram of experimental area.

fining; it was $\frac{3}{8}$ in. high by $\frac{3}{8}$ in. wide and located 103 in. from the center of the hydrogen target. Protons passing through the small solid angle subtended by counter S_2 insured that the conjugate neutrons were emitted within a small cone that could be totally intercepted by the neutron counter to be calibrated.

A differential-range curve was taken with the proton telescope (θ_p) set near 0°. A range "bite" of 2.08-g/cm^2 copper (formed by absorber A_2 and part of counter S_3) was used to give a small spread in energy to the scattered neutrons, in conjunction with a reasonable counting rate. The absorber was varied at A_1 for the range curve. The measured energy of the neutron beam was found to be 205±6 Mev at $\theta_p=30°$ and 205±3 Mev at $\theta_p=5°$. The maximum spread in energy of the scattered neutrons—obtained by folding in the geometrical effects due to beam, hydrogen target, and counter dimensions—was ±1.2 Mev at $T_n=6.8$ Mev, and ±5 Mev at $T_n=46$ Mev.

For the above incident-neutron energy, the neutron counter was placed at an angle θ_n (see Fig. 1), at which the energy of the scattered neutron coincided with that desired for the efficiency measurement. The proton telescope was then moved to the appropriate conjugate angle θ_p determined by the kinematics of n-p scattering for this energy. The appropriate change in the absorber A_1 was made for each of the neutron energies measured.

A simplified diagram of the electronics is shown in Fig. 2. A coincidence of S_1, S_2, S_3, with S_4 in anticoincidence, signals a proton of the desired energy. The output of this circuit then opens the gate G_1 at a time 16 nsec after the beam neutron entered the H_2 target. Thus, only neutrons from approximately 76 to 4 Mev can normally pass through G_1, which was 40 nsec wide. If a neutron in this range was detected by the neutron counter, its signal went through gate G_1, after which it opened gate G_2 to let the original stopping-proton signal through.

For neutron energies such that the neutron pulses were near the ends of G_1, measurements were also made with G_1 position shifted relative to the signal in order to accept any signals which might jitter outside of the gate. The stopping-proton signal was the time reference. Both signals then proceeded to a chronotron[8] where their time difference was measured. Appropriate delays for gate openings of G_1 and G_2 and for the chronotron inputs were predetermined by means of nanosecond light pulsers[9] installed in each of the counters. The results of this procedure were corroborated by subsequent actual measurements of the time of arrival of given-energy neutrons.

A diagram showing the geometry of one of the neutron counters used is shown in Fig. 3. This was one of the larger blocks tested. The scintillator is covered with approximately $\frac{1}{32}$-in.-thick shiny electropolished aluminum (trade name Alzak). The light guide coupling the scintillator to the photomultiplier (RCA 7046) is also made of Alzak.

As shown in Fig. 2, the output of the neutron-counter photomultiplier tube proceeds to a tunnel-diode discrimi-

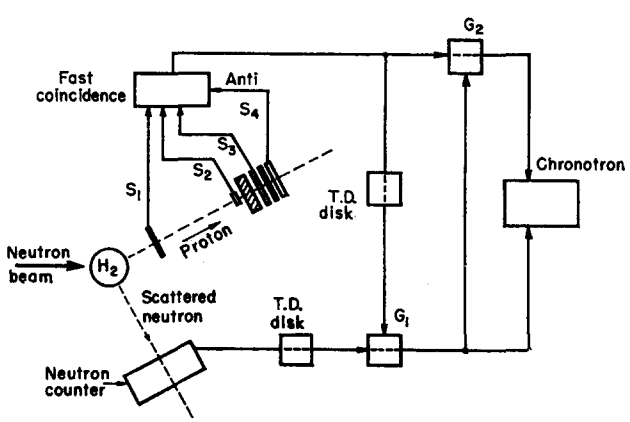

FIG. 2. Simplified schematic of electronics.

[8] A. E. Bjerke, Q. A. Kerns, and T. A. Nunamaker, Nuclear Instr. & Methods 12, 25 (1961).

[9] Tom Innes and Quentin Kerns, "Triggered nanosecond pulsed light source," Lawrence Radiation Laboratory Report UCRL-9726, August, 1961 (unpublished.)

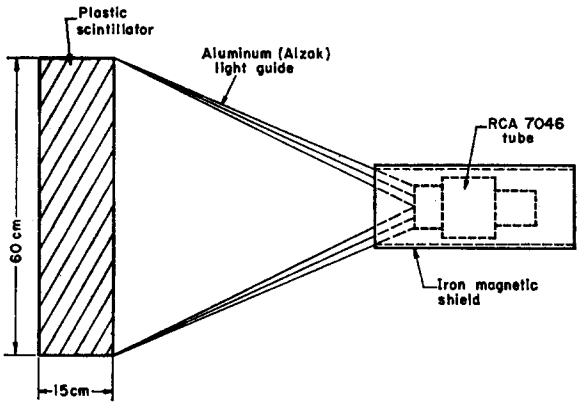

FIG. 3. Neutron counter.

nator described elsewhere.[10] The level of the discriminator—in conjunction with the high voltage on the photomultiplier—determined the bias for the counter. In order to be biased for protons of approximately 4 Mev, we demanded that the counter be able to detect $\approx 20\%$ of the 1.28-Mev γ rays from a Na^{22} source. This source was then used to calibrate other counters.

To insure that the neutron counter was geometrically intercepting the neutron flux determined by the conjugate protons in the proton telescope, the neutron counter was moved both horizontally and vertically in the plane perpendicular to the direction of the scattered neutrons until a loss in neutron flux resulted. For $\theta_p > 15°$, we found that the neutron counter intercepted all neutrons at a distance of 5 ft from the hydrogen target. For $\theta_p < 15°$ (hence neutron energies less than 15 Mev), the neutron counter was moved closer to the hydrogen target for the absolute efficiency measurement. These experimentally determined angular spreads of the scattered neutrons were in agreement with results calculated from the geometry of our apparatus.

The counting rate in the proton telescope varied as a function of angle. The average counting rate in the telescope was ≈ 1 count/sec with a range "bite" of 2.08-g/cm^2 copper in the proton telescope, and the solid angle determined by counter S_2.

III. RESULTS

The neutron efficiency for our scintillator is shown in Fig. 4 for the energy region 4.4 to 76 Mev. For these results the measured effects of the target container and of accidental events have been subtracted. The resulting errors are statistical. Most of the measurements were made with plastic scintillator A which was 15 cm thick, 20 cm high, and 60 cm wide. Three points are included with scintillator B, whose corresponding dimensions were 15×20×20 cm. As seen in Fig. 4, A and B give the same results.

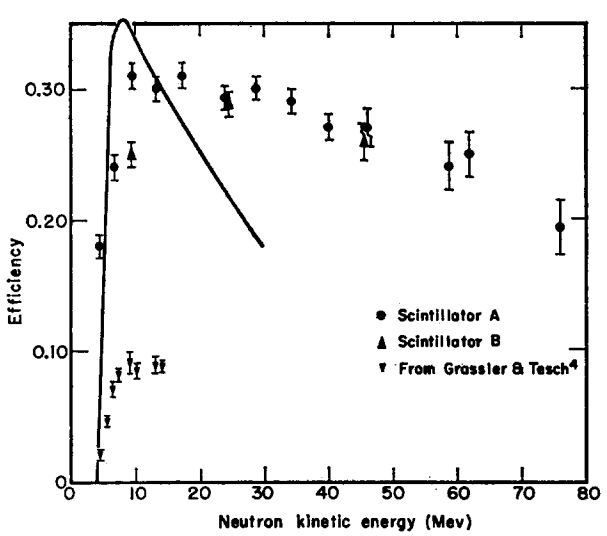

FIG. 4. Neutron counter efficiency.

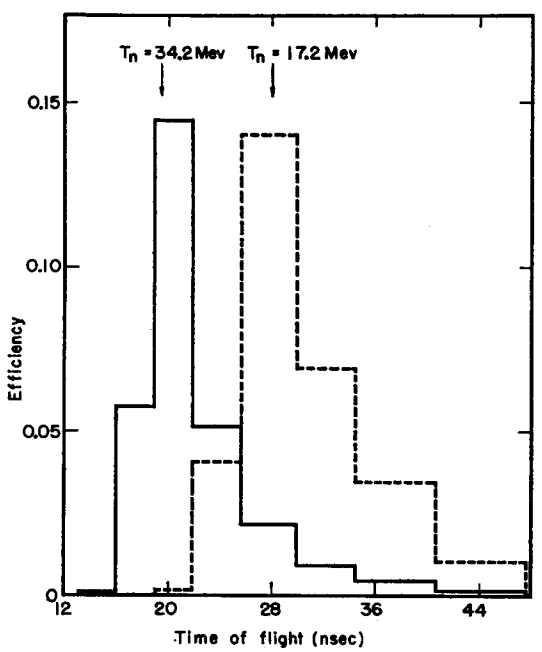

FIG. 5. Time distribution of output signals from neutron counter for two neutron energies.

The curve shown in Fig. 4 is the calculated efficiency, considering only single n-p collisions and using the n-p cross sections of Hughes and Harvey.[11] A proton bias of 4 Mev was used in the calculation. The trend of our measured efficiency seems to indicate a bias between 3 and 4 Mev, as originally anticipated. As mentioned earlier, the effect

[10] A. E. Bjerke, Q. A. Kerns, and T. A. Nunamaker, "Pulse shaping and standardizing of photomultiplier signals for optimum timing information using tunnel diodes," Lawrence Radiation Laboratory Report UCRL-9838, August 1961 (unpublished).

[11] D. J. Hughes and J. A. Harvey, "Neutron cross sections," Brookhaven National Laboratory Report BNL-325, July 1955 (unpublished).

of the carbon in the scintillator is not important below 10 Mev. Above 10 Mev its effect can be noted by the departure of our experimental points from the calculated n-p efficiency.

It is of interest to compare the results with those of Grassler and Tesch.[4] They obtained 14-Mev neutrons from the reaction T(d,n) He^4, and scattered them on a CH_2 target. Neutron efficiencies were then measured below 14 Mev in a 5-cm-thick plastic scintillator. Their results are shown in Fig. 4 for a 3.5-Mev bias. The two sets of data have very nearly the same shape and bias, but differ in magnitude by approximately a factor of 3, which is the ratio of the thicknesses of scintillators used.

In Fig. 5 the distribution of neutron counter pulses in time is shown for two neutron energies. The average flight path for the neutrons is 5.25 ft. The calculated time of flight for the mean energies indicated is shown by the arrows. The spread in time of the pulses is due to such effects as energy spread of the scattered neutrons, thickness of the neutron counter, and electronic spread from the phototube and discriminator due to light signals of varying levels in the scintillator. The integrated histograms of Fig. 5 yield the efficiencies given in Fig. 4.

ACKNOWLEDGMENTS

We wish to thank Professor Emilio Segrè for his support and interest. The support and cooperation of James Vale and the 184-in. cyclotron personnel are gratefully acknowledged.

THE REVIEW OF SCIENTIFIC INSTRUMENTS VOLUME 33, NUMBER 5 MAY, 1962

New Emission X-Ray Microscope

Y. YONEDA
Department of Applied Physics, Kyushu University, Fukuoka, Japan
(Received February 1, 1961; and in final form, February 1, 1962)

A new x-ray microscope described here uses x rays emitted by substances under electron bombardment. A pinhole formed by four knife edges is used for the projection. The purpose of this microscope is similar to that of the scanning electron microscope. The resolving power of about 0.45 μ was obtained by a comparatively simple apparatus. The construction, operation, resolution, and contrast of photographs obtained with the microscope are discussed, and, for comparison, examples of photographs are shown together with conventional optical micrographs.

I. INTRODUCTION

WHEN an optical microscope or an electron microscope is used, the structure of a sample is observed mainly by the geometrical details, the reflective power or the transparency at each part. An ordinary x-ray projection microscope reveals the structure of samples by the transparency and is capable of discriminating elements roughly. On the other hand, the electron probe microanalyzer developed recently by Castaing *et al.*[1] is used to measure the intensity and wavelength of x rays emitted by irradiating the sample surface with a fine focus electron beam. As this method enables us to know the composition of a microcomponent of a surface by Moseley's law, it is a means of rapid chemical point analysis, and may be said to be a remarkable advance. Finally, the scanning electron microscope, which yields the distribution of elements as patterns by reconstructing a point-by-point analysis, has been recently developed by Cosslett *et al.*[2] These apparatuses contribute to metallurgy and mineralogy. The present paper describes an emission type x-ray microscope. The purpose of it is similar to that of the scanning electron microscope, though it is simpler in design and operation, and different in principle.

[1] R. Castaing, J. Philibert, and C. Crussard, J. Metal **9**, 189 (1957).
[2] V. E. Cosslett and P. Duncumb, Nature **177**, 1172 (1956).

II. DESCRIPTION OF THE MICROSCOPE

1. Principle and Construction

When the sample surface is irradiated uniformly by a beam of accelerated electrons, the microcomponents of the surface emit white x rays and characteristic x rays whose intensity depends on the atomic weight. To project these x rays on an x-ray film through a pinhole set as close to the sample as possible is the principle of this microscope. The design is shown in Fig. 1. The angle between the electron beam and the surface of the sample is made to be 20°. The filament of the electron gun is a tungsten wire set parallel to the surface of the sample. The tungsten wire is 0.3 mm in diameter and 8 mm in length, and a semicircular cross section is given. The cylindrical Wehnelt cathode is 20 mm in inside diameter and 20 mm in height. A plate with a square hole 8×12 mm is placed in the cylinder. The filament is in this square hole. The necessary area of the surface of the sample is irradiated uniformly by the electron beam of this electron gun.